Radiation Physics and Chemistry 222 (2024) 111887

Contents lists available at ScienceDirect

Radiation Physics and Chemistry

journal homepage: www.elsevier.com/locate/radphyschem

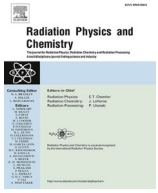

Average dose rate is the primary determinant of lipid peroxidation in liposome membranes exposed to pulsed electron FLASH beam

Veljko Grilj [a,*], Ryan Paisley [a], Kevin Sprengers [a], Walther-Reiner Geyer [a], Claude Bailat [a], Francois Bochud [a], Marie-Catherine Vozenin [b,c], Sergei Vinogradov [d,e], Pascal Froidevaux [a,**]

[a] Institute of Radiation Physics, Lausanne University Hospital, Lausanne, Switzerland
[b] Laboratory of Radiation Oncology, Radiation Oncology Service and Oncology Department, Lausanne University Hospital and University of Lausanne, Lausanne, Switzerland
[c] Radiotherapy and Radiobiology Sector, Radiation Therapy Service, University Hospital of Geneva, Geneva, Switzerland
[d] Department of Biochemistry and Biophysics, Perelman School of Medicine, University of Pennsylvania, Philadelphia, USA
[e] Department of Chemistry, School of Arts and Sciences University of Pennsylvania, Philadelphia, USA

ARTICLE INFO

Handling Editor: Dr. Jay Laverne

ABSTRACT

Background: Lipid peroxidation, a self-propagating chain reaction that oxydates lipid molecules, contributes to harmful effects of ionizing radiation. A decrease in peroxidation at higher dose rates could play a role in the FLASH sparing effect.
Purpose: We explored how lipid peroxidation induced by FLASH (>100 Gy/s) and conventional (CONV, <0.2 Gy/s) radiation depends on lipid concentration and content of polyunsaturated fatty acids (PUFA). Additionally, we investigated the correlation between the lipid peroxidation and the main beam parameters characterizing pulsed electron beams, namely the dose per pulse (DR_p) and the average dose rate (DR_{av}).
Methods: We employed phosphatidylcholine (PC) liposomes as a model of biological membranes. Suspensions of liposomes containing different proportions of linoleic acid (LA) were prepared at various concentrations and irradiated at FLASH and CONV dose rates. Additionally, the liposomes were exposed to beams characterized by diverse combinations of DR_p and DR_{av}. The extent of lipid peroxidation was assessed by monitoring oxygen consumption (ΔpO_2) and measuring the yield of malondialdehyde (MDA), and in certain instances, of lipid peroxides (LOOH).
Results: Regardless of the radiation dose, liposome concentration or LA content, ΔpO_2 and the yield of MDA were significantly lower for FLASH than for CONV irradiation. Increase in the proportion of readily oxidizable LA in the lipid had negative effect on the MDA yield but correlated positively with ΔpO_2 and LOOH yield. Exposing liposomes to beams operating at different pulse repetition frequencies, while keeping the total dose and DR_p constant, resulted in markedly different ΔpO_2 and MDA yields. In contrast, DR_{av} was found to exhibit stable correlation with both MDA yield and ΔpO_2.
Conclusions: Irradiation at FLASH dose rates produces lower yield of lipid peroxidation in PUFA-containing artificial PC membranes than CONV irradiation under all tested conditions. Time-averaged dose rate, in contrast to pulse dose rate, was the critical parameter determining the level of lipid peroxidation induced by pulsed electron beams.

1. Introduction

FLASH radiotherapy offers exciting prospects for improving cancer treatment by exploiting the differential response of normal and tumor tissues to ultra-high dose rate radiation (UHDR >100 Gy/s) (Vozenin et al., 2022; Bourhis et al., 2019). FLASH, in contrast to conventional radiotherapy (CONV), where radiation is administered at dose rates below 0.2 Gy/s, reduces the adverse radiation effects on healthy tissue while maintaining effective tumor control (Gao et al., 2022). From the radiation chemistry standpoint, two scenarios have been envisioned

* Corresponding author.
** Corresponding author.
E-mail addresses: Veljko.Grilj@chuv.ch (V. Grilj), Pascal.Froidevaux@chuv.ch (P. Froidevaux).

https://doi.org/10.1016/j.radphyschem.2024.111887
Received 1 March 2024; Received in revised form 29 May 2024; Accepted 30 May 2024
Available online 2 June 2024

when dose rates approach those typical of FLASH, potentially impacting the severity of the biological damage (Wardman, 2020). The first involves depletion of chemicals (e.g. oxygen) that are vital for biological function and response to radiation. The second refers to an increase in the rate of radical-radical interactions. While these interactions hold little significance at lower dose rates, at UHDR they can decrease the number of radicals available to react with biological structures and/or modify the kinetics of the radical chain propagation/termination.

It has long been recognized that the yield of non-enzymatic peroxidation of phospholipid membranes initiated by ionizing radiation decreases with an increase in the radiation dose rate (Mead, 1952; Hyde and Verdin, 1968; Petkau and Chelack, 1976; Nakazawa and Nagatsuka, 1980; Stark, 1991). Paralleling the second scenario mentioned above, this effect has been attributed to the dose rate-dependent recombination of radicals that results in enhanced termination of the peroxidation chain reactions at higher dose rates (Stark, 1991).

Various detrimental effects of radiation, including radiation-induced cell death (Ye et al., 2020; Lei et al., 2020; Pearson et al., 2021; Zhang et al., 2022), acute tissue injury (Li et al., 2019a, 2019b), and chronic inflammation (Zhao and Robbins, 2009) have been associated with lipid peroxidation. Moreover, malondialdehyde (MDA) and 4-hydroxynonenal (4-HNE), the breakdown products of lipid hydroperoxides (LOOH) that can engage in secondary deleterious reactions, are frequently employed to assess acute and chronic oxidative stress following irradiation (Catala, 2009; Ayala et al., 2014). Thus, producing less lipid peroxidation by use of high dose rates holds promise for partially mitigating radiation-induced injury, an effect that could be relevant in the context of FLASH-RT.

In our previous work, we have shown that irradiation of phospholipid micelles and liposomes with pulsed FLASH electron beam produces significantly lower yield of the peroxidation process compared to CONV beams (Froidevaux et al., 2023). In the present study, we continued using phosphatidylcholine (PC) liposomes as a model of biological membranes to explore the dependance of lipid peroxidation on liposome concentration and the content of polyunsaturated fatty acids (PUFA) in the lipid mixture. We implemented continuous monitoring of oxygen uptake during irradiation of liposome solutions and demonstrated better accuracy and sensitivity of this method, compared to MDA quantification, for assessing the degree of peroxidation process. Finally, we investigated how beams characterized by various combinations of pulse dose rate and time-averaged dose rate (See definitions below.) differ in terms of the resulting lipid peroxidation yield.

1.1. Mechanism of lipid peroxidation

Water radiolysis leads to the generation of several radicals, including the hydroxyl radical, $HO^{\bullet}$. This radical reacts at a diffusion-limited rate with the *bis*-allylic system of a polyunsaturated fatty acid (PUFA), such as linoleic acid, producing a carbon-centred radical, denoted as $L^{\bullet}$ (1). Subsequently, $L^{\bullet}$ can react with dioxygen, generating a lipid peroxyl radical, $LOO^{\bullet}$ (2). While $LOO^{\bullet}$ is much less reactive than $HO^{\bullet}$, it can oxidize another molecule of PUFA, leading to the formation of a new $L^{\bullet}$ radical and subsequently engaging another molecule of oxygen, thus propagating the peroxidation reaction (3). However, when concentration of $LOO^{\bullet}$ reaches high levels, two molecules of $LOO^{\bullet}$ can merge, forming an intermediate, whose splitting results in the formation of an alcohol, a ketone, and one molecule of oxygen (4 and 5). Hence, the inter-radical reaction (4) is effectively a chain termination step.

$$HO^{\bullet} + L-H \xrightarrow{k_i} L^{\bullet} + H_2O \quad k_i \approx 10^9 - 10^{10}\ \mathrm{M^{-1}\,s^{-1}} \tag{1}$$

$$L^{\bullet} + O_2 \xrightarrow{k_{perox}} LOO^{\bullet} \quad k_{perox} \approx 3 \times 10^8\ \mathrm{M^{-1}s^{-1}} \tag{2}$$

$$LOO^{\bullet} + L-H \xrightarrow{k_p} LOOH + L^{\bullet} \quad k_p \approx 1 - 100\ \mathrm{M^{-1}s^{-1}} \tag{3}$$

$$LOO^{\bullet} + LOO^{\bullet} \xrightarrow{k_t} [LOO-OOL]^{\#} \quad k_t \approx 10^5 - 10^7\ \mathrm{M^{-1}s^{-1}} \tag{4}$$

$$[LOO-OOL]^{\#} \rightarrow L-OH + LH=O + O_2 \tag{5}$$

2. Material and methods

2.1. Irradiation setup and dose delivery

Irradiations were conducted using the Oriatron eRT6 LINAC (PMB Alcen), which generated a pulsed electron beam with the energy in the range of 5–6 MeV (Jaccard et al., 2018). The physical beam parameters, such as pulse dose rate (DR_p) and time-averaged dose rate (DR_{av}), could be adjusted by regulating the pulse width (w), pulse repetition frequency (PRF), electron current and the source to surface distance (SSD). Note that DR_p here is defined as the radiation dose deposited by a single LINAC pulse (in Gy), divided by its width w (in s), where w commonly refers to the full width at half-maximum of the pulse. Conversely, time-averaged dose rate (DR_{av}) refers to the total dose deposited by a sequence of LINAC pulses divided by the duration of that sequence. Thus, for example, for a single pulse of 1Gy and w of 2μs, $DR_p = DR_{av} = 5 \times 10^5$ Gy/s. But for a sequence consisting of four such pulses, spaced by 100 μs (corresponding to PRF = 1/100 μs = 10 kHz), $DR_p = 5 \times 10^5$ Gy/s and DR_{av} = 4 Gy/400 μs = 10^4 Gy/s.

During irradiations, liposome dispersions were sealed in glass vials (Infochromag GO74B-14/19-SKFW16-H, 1.75 mL), which were immersed in a water bath, such that the vials' central axes were 10 mm from the air-water interface. The vials were centred with respect to the beam with aid of lasers. The water bath was placed on a movable platform that could be translated along the direction of the beam axis, thus allowing for adjustment of the SSD. The beam parameters used for FLASH and CONV modes are listed in Table 1.

To investigate the dependence of the lipid peroxidation yield on the beam parameters, the pulse width was set as w = 1 μs, while DR_p was adjusted in the range of 2×10^5 - 1.2×10^6 Gy/s (corresponding to dose-per-pulse, DPP, in the range of 0.02–1.2 Gy) by tuning the SSD and electron current. Different DR_{av}'s were achieved for the same DR_p by changing the PRF while maintaining the SSD constant. The range of the achieved DR_{av} values across the whole range of DR_p was 0.1–500 Gy/s. In total, 20 different combinations of DR_p and DR_{av} were used (Table 2). For all irradiations, the total dose was set at 40 Gy, except for the dose escalation experiment, where doses in the range of 10–40 Gy were employed.

2.2. Dosimetry

Doses were measured using a combination of passive and active dosimeters, including GafChromic EBT3 films, an Advanced Markus ionization chamber with correction for charge recombination (Petersson et al., 2017), and an induction coil installed at the beam exit. Initially, the ionization chamber was used to measure DPP and total dose for each beam configuration. Samples were irradiated to achieve the desired dose level based on the ionization chamber readings, while the induction coil signal was recorded for each irradiation. Alongside the samples, EBT3 films were also irradiated using the same beam configuration. After 24 h, the films were scanned and evaluated to determine the absolute doses. Using these doses as a reference, the induction coil signal was retrospectively calibrated for each beam configuration. The calibrated coil signal was then used to determine the actual dose deposited at the center

Table 1
Beam parameters characterizing irradiations by FLASH and CONV beams.

Mode	DPP (Gy)	DR_p x 10^4 (Gy/s)	PRF (Hz)	DR_{av} (Gy/s)
CONV	0.019	1.9	10	0.2
FLASH	4.940	261.7	100	564.6

Table 2
Combinations of dose per pulse (DPP), pulse dose rate (DR_p), pulse repetition frequency (PRF) and average dose rate (DR_{av}) used to investigate dependance of lipid peroxidation markers on temporal structure of pulsed electron beam.

DPP (Gy)	DR_p x 10^4 (Gy/s)	PRF (Hz)	DR_{av} (Gy/s)
0.019	1.9	5	0.1
0.019	1.9	10	0.2
0.027	2.7	5	0.1
0.027	2.7	10	0.3
0.027	2.7	25	0.7
0.026	2.6	50	1.3
0.072	7.2	5	0.4
0.073	7.3	10	0.7
0.072	7.2	50	3.6
0.068	6.8	200	13.6
0.133	13.3	5	0.7
0.140	14.0	10	1.4
0.136	13.6	50	6.8
0.131	13.1	200	26.2
0.534	53.4	5	2.7
0.545	54.5	30	16.6
0.533	53.3	200	107.9
1.208	120.8	5	6.2
1.194	119.4	200	246.3
4.940	261.7	100	564.6

of a sample, and its value was further corrected for lateral and depth dose distribution to obtain the final radiation dose delivered to the vial.

2.3. Chemicals

Crude phosphatidylcholine (PC) from egg yolk (~60% in PC), potassium dihydrogenophosphate hexahydrate (KH_2PO_4), thiobarbituric acid (TBA), trichloroacetic acid (TCA), xylenol orange (XO), ammonium iron(II) sulfate hexahydrate (Fe^{2+}), 2,6-Di-tert-butyl-4-methylphenol (BHT), perchloric acid (PCA), dimethylformamide (DMF), trimethylamine (Et_3N), lithium metal, chloroform ($CHCl_3$), n-pentanol and methanol (MeOH) were of analytical grade and purchased from Sigma Aldrich or Brunschwig Chemie (Switzerland). Phosphatidylcholine from soybean (95%) was purchased from Brunschwig Chemie (Switzerland). 2,3-dicyanonaphthalene was purchased from TCI (Belgium).

2.4. Phosphatidylcholine liposomes preparation

Phosphatidylcholine (PC) was purified immediately before liposome preparation. The purification process involved removal of phosphatidylethanolamine, tocopherol (along with other antioxidants), and various impurities, consisting mainly of free polyunsaturated fatty acids (PUFA) and saturated fatty acids. The purification was accomplished by chromatography on a silica gel column using gradient elution (MeOH in $CHCl_3$, 10 → 50%)(Zhang et al., 2003). The fractions containing PC were collected, the solvents were removed using a rotary evaporator, and the remaining solid was dried overnight under vacuum. The resulting pure PC was dissolved in $CHCl_3$, forming a stock solution for subsequent experiments. The specific PC compositions used were as follows: PC 18:2 15% (where %-value refers to the content of linoleic acid in the total fatty acids content), which was obtained from egg yolk, and PC 18:2 60%, which was obtained from soybean. Additionally, PC 18:2 35% was obtained by mixing equal molar quantities of PC 18:2 15% and PC 18:2 60%. To achieve the final concentration of 20 mM PC liposomes, an aliquot of the stock solution of PC in $CHCl_3$ was taken, the solvent was removed on a rotary evaporator, and the solid was dried under vacuum for 1 h. Subsequently, 20 mL of phosphate buffer (5 mM, pH 7.4) was added, and the mixture was left for 1 h to wet and then was subjected to sonication during 30 s. The obtained solution was diluted with the buffer to a total volume of 40 mL, vortexed thoroughly and extruded ten times under N_2 (nitrogen gas) atmosphere through a polycarbonate membrane (100 nm average pore size) using a Genizer JGE-100 mL liposome extruder (Genizer LLC, CA, USA). The resulting liposomes were stored at 4 °C and used within 24 h. The size distribution of the liposomes was determined by dynamic light scattering using a Delsa Nano C apparatus (Beckman-Coulter). The liposomes were found to exhibit an average diameter of 100 ± 20 nm (n = 6) and polydispersity index of 0.08. In all experiments, irradiations were conducted using liposome solutions that were equilibrated with the air (containing 21% O_2).

2.5. Assessment of lipid peroxidation

2.5.1. Determination of oxygen uptake during irradiation

Oxygen concentration in sealed vials subjected to radiation was measured by the phosphorescence quenching method, using molecular oxygen probe Oxyphor PtG4 (1 μM)(Lebedev et al., 2009; Esipova et al., 2011) and a commercial fiber-optic phosphorometer (Oxyled, Oxygen Enterprises), as described previously (Cao et al., 2021; El et al., 2022; Van Slyke et al., 2022). The lifetime of the phosphorescence emitted by the probe, which was dissolved directly in the medium, is dependent on the oxygen concentration, or partial pressure (pO_2), in the medium. pO_2 was recorded (in units of mmHg) before, during, and after irradiation with a measurement frequency of 4 Hz. The amount of oxygen consumed during irradiation of liposome samples was determined as the difference (ΔpO_2) in oxygen levels before and immediately after irradiation and expressed in units of mmHg.

2.5.2. Determination of malondialdehyde (MDA) by HPLC

To halt lipid peroxidation in both irradiated and non-irradiated (blank) samples, a solution of BHT in DMF (20 μL, 0.5 M) was added to a sample, and the mixture was vortexed to ensure its homogeneity. Subsequently, an aliquot (200 μL) of the mixture was transferred to an Eppendorf tube (0.5 mL), a solution of TBA (200 μL, 10 mM in 7.5% TCA) was added, and the mixture was vortexed for 30 s. The mixture was centrifuged at 12300 g for 20 min. The supernatant (350 μL) was transferred to a glass vial (2.5 mL), and the vial was heated and kept at 95 °C for 1 h using a heating block (Fisherbrand Isotemp). An MDA-TBA pink adduct formed, and it was isolated by HPLC (Thermo scientific UltiMate 3000) on a reverse-phase column (Lichrospher® 100 RP 10, 5 μm, n° 528600) using a mixture of phosphate buffer (100 mM, pH 6.8, 600 mL)) and Et_3N solution in MeOH (0.2%, 400 mL) at pH of 6.8 as an eluent. The product was detected by absorption at 532 nm. A calibration curve was constructed with TMP at 0.3, 0.6, 1.0, 1.5 and 2.0 μM, following the same protocol as for samples. The net MDA concentrations were calculated by subtracting the average MDA concentration obtained on at least three blank replicates from the MDA concentration of the samples.

2.5.3. Determination of lipid hydroperoxides

Lipid hydroperoxides (LOOH) were quantified as described by Gay and Gebicki (2003). In brief, LOOH were extracted from irradiated solution (200 μL) using MeOH/$CHCl_3$ (1:2, 900 μL), and the resulting mixture was subjected to centrifugation (12300 g). H_2O_2 produced during irradiation remained in the aqueous phase, while LOOH concentrated in the organic phase. An aliquot of the organic phase (400 μL) was collected into a glass vial (2 mL) and evaporated to dryness under a stream of N_2. Next, $CHCl_3$ (4 mM in BHT, 250 μL), MeOH (4 mM in BHT, 400 μL), PCA (2M, 41 μL), XO (5 mM, 30 μL), and Fe^{2+} (5 mM, 20 μL) were added to the dried sample. The mixture was then incubated at room temperature for 1 h, then the Fe^{3+}-XO complex absorbance was measured at 560 nm (Thermo Fisher Evolution 200) in 1 cm glass cuvette. The absorbance at 560 nm directly correlated with the concentration of LOOH, after subtracting the average absorbance obtained from at least three blank replicates.

2.5.4. Determination of post irradiation oxygen uptake by EPR oximetry

To determine oxygen uptake by lipid suspensions over extended periods of time (hours) after irradiation, we employed electron

paramagnetic resonance (EPR) oximetry with lithium naphthalocyanine crystal (LiNc) as a probe (Pandian et al., 2009). This method is based on the ability of O_2 to quench electron spin polarization, whereby the linewidth of the radical probe signal correlates with oxygen concentration in the environment.

LiNc was prepared according to Pandian et al. (2009). Briefly, a mixture of methanol (4 mL) and n-pentanol (36 mL) containing lithium metal (0.2 g) was refluxed under nitrogen for 3 h. After cooling the mixture to room temperature, 2,3-dicyanonaphthalene (1.2 g, 6.7 mmol) was added, and the mixture was refluxed until 2,3-dicyanonaphthalene was completely consumed. The reaction mixture was filtered and left on air overnight. A bluish material was obtained upon evaporation of the solvent on a rotary evaporator. The material was washed with dry acetone and with methanol–THF (1:1 v/v). The dark bluish-green insoluble material, LiNc, was collected by filtration and dried under vacuum in a desiccator (yield 35%).

The calibration of the LiNc peak-to-peak EPR linewidth as a function of the concentration of molecular oxygen was conducted using independent O_2 concentration measurements with an OxyLite Pro XL instrument (Oxford Optronix, UK). These measurements were taken using phosphate buffer solutions containing LiNc, which were either fully saturated with O_2 or partially saturated with O_2 by introducing argon (Ar). LiNc powder (1 mg) was combined with phosphate buffer (5 mM, 100 μL), and 50 μL of the resulting slurry was added to PC 18:2 15% (10 mM, 1.75 mL) in a glass vial. The mixture was then vortexed for 30 s to ensure thorough mixing. An additional 50 μL of the prepared slurry was transferred into a capillary tube, which was sealed at both ends using paraffin wax. This capillary tube was then subjected to measurements to determine the O_2 concentration before initiating the irradiation process.

Following the irradiation of the 1.75 mL glass vial, another capillary tube was prepared to assess the O_2 concentration immediately after irradiation and at various intervals over a period of several hours. EPR measurements were performed using a Bruker EMX Nano spectrometer (Bruker, Germany), with the following parameters: frequency: 9.653 GHz, centre field: 3444 G, scan width: 110 G, scan time: 30 s, number of scans: 2, receiver gain: 40 dB, modulation amplitude: 1 G, and attenuation: 10 dB (10 mW microwave power), conv time: 30 ms, number of points: 1000.

2.6. Statistical analysis

2.6.1. Oxygen measurements

The average oxygen consumption during irradiation was determined by subtracting the average oxygen pressure values calculated over 5 s before and after the irradiation. The standard deviation for this calculation was obtained by propagating the standard deviations of the average oxygen values before and after irradiation.

2.6.2. MDA and LOOH measurements

Uncertainties on MDA and LOOH concentration were calculated as a propagation of several individual A-type uncertainties given by i) HPLC or UV-VIS calibration: 5% ii) dilutions: 2% iii) MDA-TBA synthesis yield: 5% iv) initial LA and PC concentrations: 4%. Considering additional systematic uncertainties (positioning, O_2 level, temperature variations, etc.), an overall uncertainty of at least 10% for MDA and LOOH dosages must be considered for every measure. Overall uncertainty on the irradiation dose was ~5%. (k = 2).

2.6.3. EPR measurements

Uncertainties on oxygen concentration measured by EPR were calculated as a propagation of several individual A-type uncertainties given by i) OxyLite Pro XL O_2 calibration: 5% ii) dilutions: 2% iii) EPR line width measurement: 3% iv). Considering additional systematic uncertainties (positioning, cavity tuning, temperature variations, etc.), an overall uncertainty of 10% for O_2 determination by EPR oximetry must be considered for every measure.

3. Results

3.1. Dependance of lipid peroxidation on liposome concentration and content of PUFA

We investigated lipid peroxidation in PC liposome samples induced by 40 Gy of radiation delivered at CONV and FLASH dose rates (beam parameters defined in Table 1) as a function of the liposome concentration. The extent of the oxidation was assessed by measuring both ΔpO_2 and MDA production. A representative time course of oxygen depletion in irradiated liposome solution is shown in Fig. 1. Measurements of ΔpO_2 and MDA at various liposome

concentrations were performed using liposomes composed of PC lipids with three different contents of polyunsaturated linoleic acid (LA). The results of these measurements are shown in Fig. 2. Oxygen consumption upon CONV irradiation exhibits a significant increase with liposome concentration for all three liposome compositions (Fig. 2A). This effect is higher for liposomes containing 35% and 60% of LA, where the observed ΔpO_2 values are close. Liposomes containing the lowest LA content (15%) consume 30%–45% less oxygen, depending.

on the liposome concentration, compared to the liposomes with higher LA contents. Oxygen consumption induced by FLASH irradiation is considerably lower for all liposome concentrations, and there is no distinction between liposomes with different LA content.

MDA production induced by CONV irradiation also exhibits a positive correlation with the liposome concentration (Fig. 2B). However, in contrast to oxygen consumption, the highest MDA yield is observed in liposomes with the lowest content of LA. The negative correlation between the LA content and MDA formation suggests that the mechanism of oxidation and/or reaction propagation in liposomes with higher LA contents might differ from that in liposomes with lower LA contents (explanation proposed in Discussion). Nevertheless, MDA yields were consistently lower for FLASH than for CONV irradiation. These findings, combined with the oxygen consumption results, show that radiation delivered as FLASH results in reduced level of lipid peroxidation irrespective of the liposome composition and concentration.

Plotting MDA concentration against ΔpO_2 (Fig. 3) makes it clear that FLASH irradiation, compared to CONV irradiation, consistently leads to lower O_2 consumption and MDA production. In addition, ΔpO_2 appears to correlate with MDA production. However, while using PC with low LA content (15%) yields the highest MDA concentrations, it does not result in the highest ΔpO_2's, which is consistent with the observation displayed in Fig. 2. The opposite behavior is observed for PC with 60% LA.

The point where MDA production reaches zero does not coincide with zero oxygen consumption, for both FLASH and CONV. This observation emphasizes that 40 Gy of radiation applied to a phosphate buffer alone already leads to oxygen consumption, presumably *via* its reduction by aqueous electrons and hydrogen atoms with end formation of hydrogen peroxide (after disproportionation of superoxide). In fact, irradiation (40 Gy) of the phosphate buffer alone yielded ΔpO_2 of

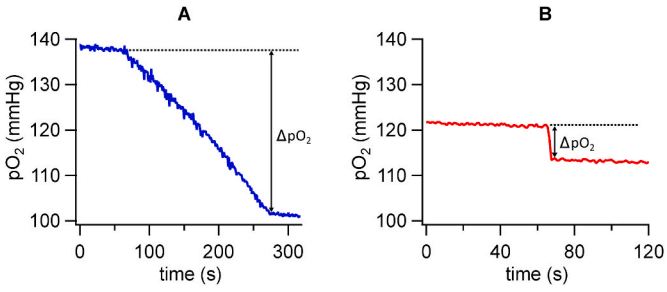

Fig. 1. Oxyphor oxygen sensitive probe allows for precise time resolved monitoring of oxygen partial pressure in closed liposome samples. Time course of oxygen depletion in 5 mM PC liposome solution irradiated with 40 Gy of **(A)** CONV and **(B)** FLASH.

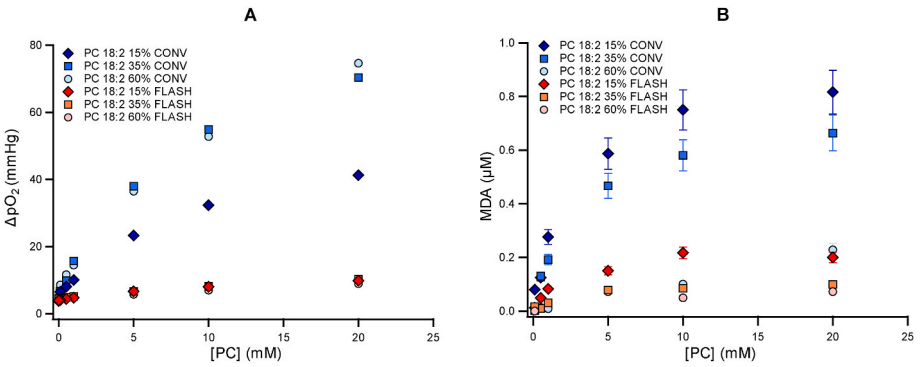

Fig. 2. FLASH radiation leads to lower lipid peroxidation yields than CONV radiation regardless of liposome concentration or PUFA content. **(A)** oxygen consumption and **(B)** MDA production after 40 Gy of CONV or FLASH (Table 1) as a function of PC liposome concentration. The results are displayed for liposomes with 15%, 35%, and 60% LA content.

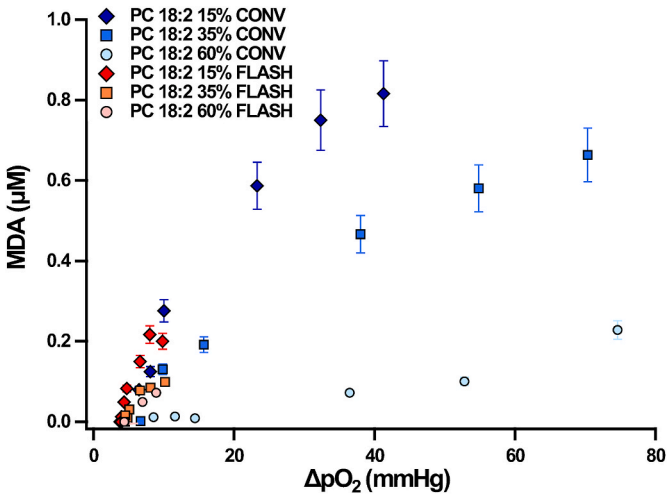

Fig. 3. MDA production as a function of O_2 consumption (ΔpO_2) after 40 Gy irradiation of solutions having various liposome concentrations (0.1–20 mM). The results are shown for liposomes containing 15%, 35% and 60% of LA.

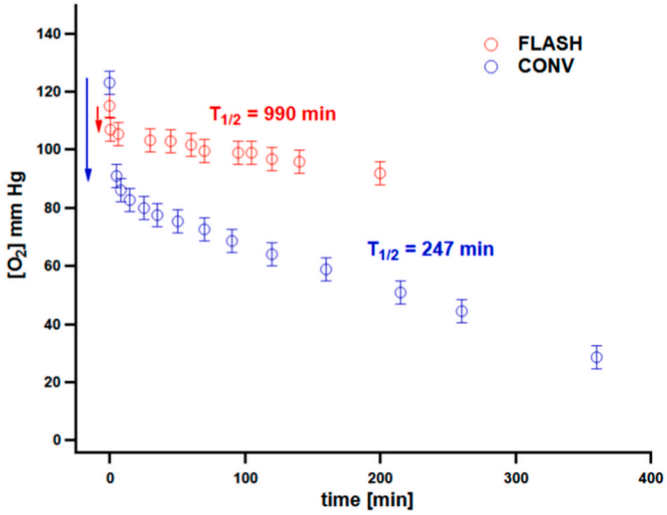

Fig. 4. Following CONV irradiation, the lipid peroxidation process persists for hours at a higher rate compared to the rate observed after FLASH irradiation. Time dependance of oxygen concentration in a sealed 50 μL glass capillary containing 10 mM PC (18:2 15%) liposome solution irradiated (30 Gy) by FLASH (red square) and CONV (blue circle). Arrows indicate change in oxygen during the irradiation.

3.5–4.5 mm Hg, depending on the irrradiation mode used.

3.2. Post irradiation oxygen consumption measured by EPR oximetry

EPR oximetry using LiNc was utilized to observe long-term oxygen consumption after irradiation. The initial oxygen consumption measured by this method and derived from the recorded pO_2 values immediately before and after the irradiation was notably higher for CONV compared to FLASH dose rates (Fig. 4). This observation is in line with the results obtained from the oxygen measurements by phosphorescence during irradiation (Figs. 2 and 3). Importantly, long-term O_2 monitoring revealed that CONV irradiation induced oxygen consumption that continued long after irradiation was stopped, suggesting that the peroxidation process terminated only after all available oxygen was consumed. In contrast, FLASH irradiation led to a much less oxygen consumption over an extended period. Based on the slopes of the respective plots (Fig. 4), we estimated by extrapolation the time required to consume half of the available oxygen in the EPR tube to be 247 min for CONV and 990 min for FLASH.

3.3. Dependance of lipid peroxidation on radiation dose

To investigate the dose dependence of the differential effect of CONV and FLASH on lipid peroxidation, we conducted a dose-response study, measuring oxygen consumption and MDA production simultaneously. The samples consisted of PC liposomes (10 mM) with varying contents of LA, which were exposed to radiation doses ranging from 5 Gy to 40 Gy. In the case of CONV irradiation, a dose-dependent increase in ΔpO_2 and MDA yield was observed across all samples, as shown in Fig. 5. However, a reduction in MDA production was evident once again for liposomes with a higher content of LA. Both MDA and ΔpO_2 increased much less with the dose for FLASH compared to CONV experiments, revealing that the difference in lipid peroxidation induced by FLASH vs CONV persists at all doses.

3.4. Dependance of lipid peroxidation on temporal characteristics of pulsed electron beam

One of the main goals of our study was to investigate the dependance of the degree of lipid peroxidation on the temporal structure of the pulsed electron beam. In particular, we aimed to elucidate whether the DR_p (the dose rate calculated for a single electron pulse) or the DR_{av} (the dose rate calculated by averaging the total dose contained in all delivered pulses over the entire time of the irradiation) is the key determinant of the degree of peroxidation induced by radiation. In this regard, we exposed PC liposomes containing 15% and 60% of LA to different

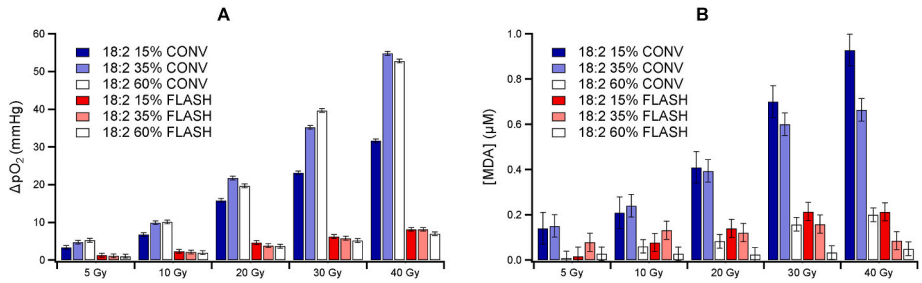

Fig. 5. FLASH produces less lipid peroxidation than CONV at all doses up to 40 Gy. The amount of **(A)** oxygen consumed and **(B)** MDA produced by irradiation of a dispersion of PC liposomes (10 mM) containing 15%, 35% and 60% LA at CONV (blue) and FLASH (red) dose rates.

combinations of DR_p and DR_{av}. As in the other experiments, we assessed the degree of lipid peroxidation by measuring ΔpO_2 and MDA production. The dependencies of these two endpoints on DR_p and DR_{av} are shown in Fig. 6. The results clearly demonstrate that DR_{av} is a much better predictor of the degree of lipid peroxidation.

3.5. Comparison of MDA and LOOH yields at various dose rates

Intrigued by the observed inverse relationship between the MDA yield and LA content, we sought to explore whether the main product of lipid peroxidation, namely LOOH, also exhibits the same trend. However, we encountered a challenge in measuring LOOH using the FOX method (Pandian et al., 2009) in the samples that contain the Oxyphor probe because of the overlapping absorbance bands of Oxyphor and the Fe^{3+}-XO complex. To overcome this limitation, we conducted an additional series of irradiations with varying dose rates and doses per pulse while measuring MDA and LOOH yields in each sample. Fig. 7 illustrates the dependence of MDA and LOOH yields on DR_{av}, which we confirmed to be a reliable predictor of the extent of peroxidation process (Fig. 6). Both measured endpoints exhibited an inverse dose rate dependence. However, it was found that the liposome membranes with the lowest LA content (15%), showed a significantly higher MDA yield and a considerably lower LOOH yield compared to liposomes with a higher LA content (60%).

4. Discussion

The results of our experiments revealed that irrespectively of the dose, liposome concentration and PUFA content, the extent of lipid peroxidation induced by FLASH is much lower than that induced by isodoses of CONV, confirming the results of our recently published work (Jaccard et al., 2018). In addition, we found that the yield of MDA was inversely proportional to the content of easily oxidizable LA, which was the most abundant PUFA in our synthetic liposome membranes. This effect was observed consistently in all experiments involving various PC concentrations (Figs. 2B and 3), radiation doses (Fig. 5B) and dose rates (Fig. 6C and D), implying that the endoperoxide formation, which is an obligatory step in the MDA generation, correlates negatively with the

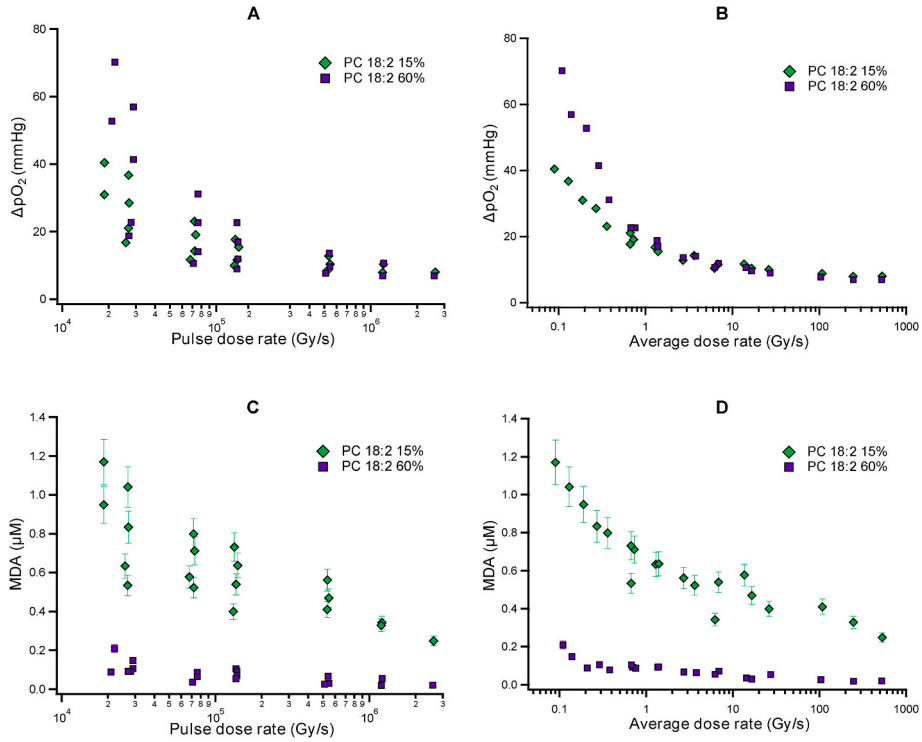

Fig. 6. The critical factor determining the yield of lipid peroxidation is the average dose rate, as opposed to the pulse dose rate. Oxygen consumption in dispersions of PC liposomes (10 mM), with two different compositions: 15% LA (green) and 60% LA (purple), plotted against **(A)** pulse dose rate DRp and **(B)** average dose rate DRav. MDA production in 10 mM dispersions of PC liposomes, with two different compositions: 15% LA (green) and 60% LA (purple), plotted against **(C)** pulse dose rate DRp and **(D)** average dose rate DRav. Vertical groups of points in **(A)** and **(C)** represent measurements obtained for similar DRp but different DRav relised by variation of PRF.

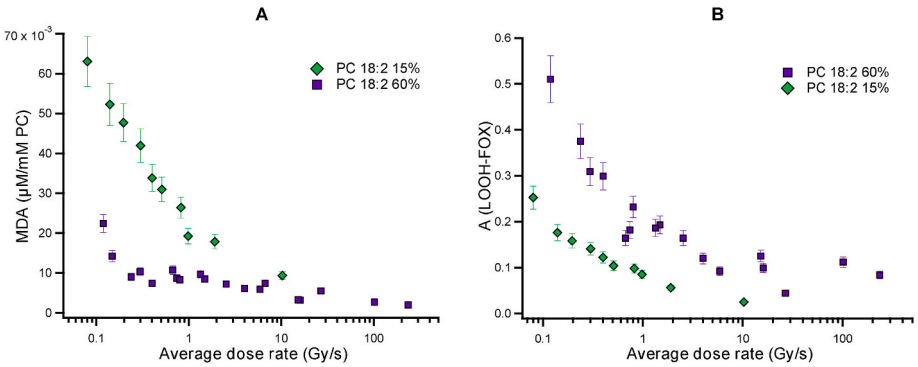

Fig. 7. MDA concentration **(A)** and LOOH-FOX absorbance **(B)** in function of the average dose rate (Gy/s) in PC liposomes (10 mM) PC 18:2 15% (green diamonds) or PC 18:2 60% (purple squares).

number of PUFA molecules within the liposome membrane. In contrast, oxygen consumption (Figs. 2A, 3 and 5A and 6B) correlated positively with the LA content, suggesting that the peroxidation chain reaction was propagating with the lowest efficiency in the membranes with the lowest LA content (15%). Similar to ΔpO_2, the yield of LOOH correlated positively with the LA content, regardless of the radiation dose rate (Fig. 7B). The association between ΔpO_2 and the production of LOOH could be expected, as LOOH is generated through the addition of O_2 to the alkyl radical, followed by propagation of the lipid peroxidation reaction and the subsequent abstraction of the bis-allylic H-atom from a neighboring PUFA.

The aforementioned findings provide a unique insight into the intricate relationship between the content of easily oxidizable PUFA, formation of endoperoxides, and the propagation of the peroxidation reaction in liposome membranes. In phospholipid membranes, the mobility of individual lipid molecules is restricted. If a lipid peroxyl radical was formed far apart from another lipid containing a bis-allylic fragment (such as in PUFA), it would preferentially form an endoperoxide (Fig. 8A) and thus terminate the chain, despite the endoperoxide formation being less thermodynamically favored. Since formation of endoperoxide is an obligatory step

in the reaction sequence leading to MDA, we hypothesize that in liposome membranes containing lower levels of highly oxidizable lipids (such as LA), and hence characterized by larger distances between individual PUFA molecules, chain termination and formation of MDA would be a more likely scenario, causing lower propagation rate and lower oxygen consumption. On the other hand, in liposome membranes with a high content of PUFA, and closer distances between PUFA molecules, the intermolecular chain propagation step (Fig. 8B) would be more probable, leading to lower yields of MDA, but higher yields of LOOH and higher oxygen consumption. Accordingly, ΔpO_2 and LOOH concentrations should be a more accurate indicator of the lipid peroxidation yield, while MDA concentrations serve as markers of intramolecular vs intermolecular reactions (Fig. 8).

The rise in ΔpO_2 and formation of MDA decelerates at higher PC concentrations (Fig. 2). Since the PC concentration is evidently not a limiting factor, initially we directed our attention to the availability of oxygen. To investigate the dependance of the peroxidation yield on O_2 concentration, we performed repetitive irradiations (20 Gy) of liposome samples (20 mM PC) in sealed glass vials. Oxygen consumption (ΔpO_2,

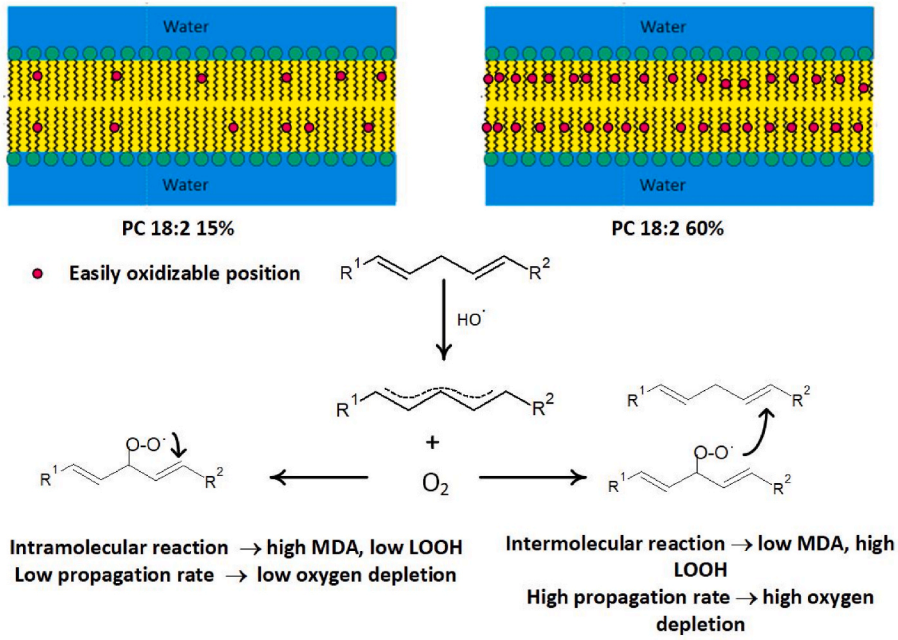

Fig. 8. Schematic representation of lipid peroxidation reactions in membranes with low (left) and high (right) PUFA content, highlighting intra- and intermolecular processes that result in endo- and exoperoxides, respectively. Initially, a delocalized radical is formed, which then adds oxygen at a diffusion-limited rate, creating a lipid peroxyl radical, typically at the C-11 position (albeit C-9 and C-13 are also possible). In the absence of an easily oxidizable site in a neighboring molecule, the peroxyl radical will react intramolecularly.

not shown) remained constant in the pO_2 range of 15–150 mmHg. Thus, the rate of the peroxidation reaction is sustained even at rather low levels of oxygen (15 mmHg), and, therefore, oxygen availability is not the root cause of the nonlinear dependence (flattening) of oxygen consumption and MDA yield on PC concentration (Fig. 2).

The flattening of the lipid peroxidation yield curve with an increase in the PC concentration could be caused by the rising rate of the termination step (reactions 4 and 5). At a constant radiation dose, the number of $HO^{\bullet}$ radicals produced by water radiolysis is constant. However, as the concentration of liposomes increases, there is higher likelihood of $HO^{\bullet}$ radicals encountering liposomes, leading to higher concentrations of $LOO^{\bullet}$ formed *via* bis-allylic H-atom abstraction and subsequent O_2 addition (Eqs (1)–(3)). Concurrently, the number of the primary radicals ($HO^{\bullet}$, $e/H^{\bullet}$) that recombine and generate H_2O, H_2O_2 and H_2 decreases. Since $LOO^{\bullet}$ is a much less potent oxidant than $HO^{\bullet}$ and reacts with lipids at a substantially lower rate, it accumulates in the membrane, which favors the termination steps (Eqs (4) and (5)).

To determine the effect(s) of the beam temporal properties on the yield of lipid peroxidation, PC liposomes with high (60%) and low (15%) LA contents were subjected to irradiations at various combinations of the pulse dose rate (DR_p) and the average dose rate (DR_{av}). Both dose rates, even though defined on different time scales, are significantly higher for a FLASH beam than for a typical CONV beam, which potentially could result in a higher instantaneous generation of radicals and subsequently higher probability of the radical recombination and chain termination processes. However, our findings revealed that DR_p is not a good predictor of the peroxidation yield. When plotted as a function of DR_p, the peroxidation yield values cluster around vertical lines, corresponding to similar DR_p but different DR_{av} (Fig. 6A and C). Therefore, for the same total dose and DR_p, ΔpO_2 and MDA production can vary significantly depending on the DR_{av}. In contrast, when plotted against DR_{av}, the values of the peroxidation yield (expressed e.g. as ΔpO_2) fall on a smooth line, showing that DR_{av} is a good predictor of the lipid peroxidation yield induced by pulsed electron beam (Fig. 6B and D). Lipids with a higher proportion of LA once more displayed elevated oxygen consumption and reduced MDA yield, aligning with the findings depicted in Figs. 1–3. Interestingly, both markers of the lipid peroxidation process reach their lowest points at DR_{av} of 10–100 Gy/s, coinciding with the minimum DR_{av} values necessary for the FLASH effect. (While our work was in progress, a study was published by Sunnerberg et al. (2023) suggesting that oxygen consumption by solutions of albumin induced at FLASH dose rates also correlates with DR_{av} rather than with DR_p).

Our studies using artificial PC membranes indicate that DR_{av}, as opposed to DR_p, correlates with oxidative degradation of PUFA-containing lipid membranes exposed to pulsed electron beams. However, artificial membranes do not represent the complexity of real biological membranes, where proteins and antioxidants, particularly tocopherol, are intimately incorporated into the PC bilayer and may play an essential role in protecting the membrane against oxidation together with other reducing agents and antioxidative enzymes that are present in the cytoplasm. Nevertheless, the fundamental features of the propagation and termination of the oxidative damage of lipid membranes are most likely to be adequately captured in experiments utilizing artificial lipid vesicles (liposomes). As such, our results suggest that lowering lipid peroxidation at FLASH dose rates might be an important component of the FLASH sparing effect *via* safeguarding healthy tissues from the adverse effects of the oxidative degradation of biological membranes.

CRediT authorship contribution statement

Veljko Grilj: Writing – review & editing, Writing – original draft, Supervision, Methodology, Investigation. **Ryan Paisley:** Writing – review & editing, Investigation. **Kevin Sprengers:** Writing – review & editing, Investigation. **Walther-Reiner Geyer:** Writing – review & editing, Investigation. **Claude Bailat:** Writing – review & editing, Supervision, Methodology, Investigation, Funding acquisition. **Francois Bochud:** Writing – review & editing, Supervision, Funding acquisition. **Marie-Catherine Vozenin:** Writing – review & editing, Funding acquisition. **Sergei Vinogradov:** Writing – review & editing, Supervision, Methodology, Investigation, Funding acquisition. **Pascal Froidevaux:** Writing – review & editing, Writing – original draft, Supervision, Methodology, Investigation, Funding acquisition.

Declaration of competing interest

The authors declare that they have no known competing financial interests or personal relationships that could have appeared to influence the work reported in this paper.

Data availability

Data will be made available on request.

Acknowledgement

The study was supported by grants of the Swiss National Science Foundation MAGIC - FNS CRS II5_186369 (to FB and MCV to support VG, WRG, KS, RP) and of National Institutes of Health P01CA244091-01 (to MCV to support VG). SV acknowledges support of the grant EB028941 from the NIH USA.

References

Ayala, A., Muñoz, M.F., Argüelles, S., 2014. Lipid peroxidation: production, metabolism, and signaling mechanisms of malondialdehyde and 4-hydroxy-2-nonenal. Oxid. Med. Cell. Longev. 360438.
Bourhis, J., Montay-Gruel, P., Gonçalves Jorge, P., et al., 2019. Clinical translation of FLASH radiotherapy: Why and how? Radiother. Oncol. 139, 11–17.
Cao, X., Zhang, R., Esipova, T., et al., 2021. Quantification of oxygen depletion during FLASH irradiation in vitro and in vivo. Int. J. Radiat. Oncol. Biol. Phys. 111 (1), 240–248.
Catala, A., 2009. Lipid peroxidation of membrane phospholipids generates hydroxy-alkenals and oxidized phospholipids active in physiological and/or pathological conditions. Chem. Phys. Lipids 157 (1), 1–11.
El, Khatib M., Van Slyke, A.L., Velalopoulou, A., et al., 2022. Ultrafast tracking of oxygen dynamics during proton FLASH. Int. J. Radiat. Oncol. Biol. Phys. 113 (3), 624–634.
Esipova, T., Karagodov, A., Miller, J., et al., 2011. Wo new "protected" oxyphors for biological oximetry: properties and Application in tumor imaging. Anal. Chem. 83 (22), 8756–8765.
Froidevaux, P., Grilj, V., Bailat, C., et al., 2023. FLASH irradiation does not induce lipid peroxidation in lipids micelles and liposomes. Rad Phys Chem 205 (11073).
Gao, Y., Liu, R., Chang, C.W., et al., 2022. A potential revolution in cancer treatment: a topical review of FLASH radiotherapy. J. Appl. Clin. Med. Phys. 23, e13790.
Gay, C.A., Gebicki, J.M., 2003. Measurement of protein and lipid hydroperoxides in biological systems by the ferric-xylenol orange method. Anal. Biochem. 315 (1), 29–35.
Hyde, S.M., Verdin, D., 1968. Oxidation of methyl oleate induced by 60Co γ-radiation. Part 1. Pure methyl oleate. Trans. Faraday Soc. 64, 144–154.
Jaccard, M., Durán, M.T., Petersson, K., et al., 2018. High dose-per-pulse electron beam dosimetry: Commissioning of the Oriatron eRT6 prototype linear accelerator for preclinical use. Med. Phys. 45, 863–874.
Lebedev, A.Y., Cheprakov, A.V., Sakadžić, S., et al., 2009. Dendritic phosphorescent probes for oxygen imaging in biological systems. ACS Appl. Mater. Interfaces 1 (6), 1292–1304.
Lei, G., Zhang, Y., Koppula, P., et al., 2020. The role of ferroptosis in ionizing radiation-induced cell death and tumor suppression. Cell Res. 30, 146–162.
Li, X., Duan, L., Yuan, S., et al., 2019a. Ferroptosis inhibitor alleviates radiation-induced lung fibrosis (RILF) via down-regulation of TGF-β1. J. Inflamm. 16 (11).
Li, X., Zhuang, X., Qiao, T., 2019b. Role of ferroptosis in the process of acute radiation-induced lung injury in mice. Biochem. Biophys. Res. Commun. 519 (2), 240–245.
Mead, J.F., 1952. The irradiation-induced Autoxidation of linoleic acid. Science 115, 470–472.
Nakazawa, T., Nagatsuka, S., 1980. Radiation-induced lipid peroxidation and membrane permeability in liposomes. Int. J. Radiat. Biol. Relat. Stud. Phys. Chem. Med. 38 (5), 537–544.
Pandian, R.P., Dolgos, M., Marginean, C., et al., 2009. Molecular packing and magnetic properties of lithium naphthalocyanine crystals: hollow channels enabling permeability and paramagnetic sensitivity to molecular oxygen. J Mater Chem. 19 (24), 4138–4147.
Pearson, A.N., Carmicheal, J., Jiang, L., et al., 2021. Contribution of lipid oxidation and ferroptosis to radiotherapy efficacy. Int. J. Mol. Sci. 22 (22), 12603.

Petersson, K., Jaccard, M., Germond, J.F., et al., 2017. High dose-per-pulse electron beam dosimetry - a model to correct for the ion recombination in the Advanced Markus ionization chamber. Med. Phys. 44, 1157–1167.
Petkau, A., Chelack, W.S., 1976. Radioprotective effect of superoxide dismutase on model phospholipid membranes. Biochim. Biophys. Acta, Biomembr. 433 (3), 445–456.
Stark, G., 1991. The effect of ionizing radiation on lipid membranes. Biochim. Biophys. Acta, Biomembr. 1071 (2), 103–122.
Sunnerberg, J.P., Zhang, R., Gladstone, D.J., et al., 2023. Mean dose rate in ultra-high dose rate electron irradiation is a significant predictor for O_2 consumption and H_2O_2 yield. Phys. Med. Biol. 68 (16), 165014.
Van Slyke, A.L., El Khatib, M., Velalopoulou, A., et al., 2022. Oxygen monitoring in model solutions and in vivo in mice during proton irradiation at conventional and FLASH dose rates. Rad Res 198 (2), 181–189.
Vozenin, M.C., Bourhis, J., Durante, M., 2022. Towards clinical translation of FLASH radiotherapy. Nat. Rev. Clin. Oncol. 19 (12), 791–803.
Wardman, P., 2020. Radiotherapy using high-Intensity pulsed radiation beams (FLASH): a radiation-Chemical Perspective. Rad Res 194 (6), 607–617.
Ye, L.F., Chaudhary, K.R., Zandkarimi, F., et al., 2020. Radiation-induced lipid peroxidation triggers ferroptosis and synergizes with ferroptosis inducers. ACS Chem. Biol. 15 (2), 469–484.
Zhang, W., He, H., Feng, Y., Da, S., 2003. Separation and purification of phosphatidylcholine and phosphatidylethanolamine from soybean degummed oil residues by using solvent extraction and column chromatography. J. Chromatogr. B 798 (2), 323–331.
Zhang, X., Li, X., Zheng, C., et al., 2022. Ferroptosis, a new form of cell death defined after radiation exposure. Int. J. Radiat. Biol. 98 (7), 1201–1209.
Zhao, W., Robbins, M.E., 2009. Inflammation and chronic oxidative stress in radiation-induced late normal tissue injury: therapeutic implications. Curr. Med. Chem. 16 (2), 130–143.